Int. J. Heat Mass Transfer. Vol. 29, No. 3, pp. 451–461, 1986
Printed in Great Britain

0017–9310/86 $3.00 + 0.00
Pergamon Press Ltd.

Turbulent heat transport in a horizontal fluid layer heated internally and from below

Y. KIKUCHI, T. SHIOYAMA and Z. KAWARA
Department of Nuclear Engineering, Kyoto University, Yoshida, Sakyo-ku, Kyoto 606, Japan

(*Received* 8 *July* 1985 *and in final form* 20 *September* 1985)

Abstract—Measurements were taken of the fluid velocity and temperature fluctuations with turbulent thermal convection in a horizontal layer of water with uniform volumetric energy sources and a constant rate of bottom heating. The experimental data were compared with a simple mixing-length analysis and a correlation equation was derived for the turbulent velocity at the midplane of the fluid layer. Turbulent heat flux, which was obtained from the measured values of velocity and temperature fluctuations, was lower than the total heat flux predicted from both internal and external heating rates.

INTRODUCTION

THERMAL convection driven by distributed volumetric energy sources is widely encountered in many scientific and engineering fields. For example, convective heat transfer with a heat-generating fluid is often considered in astrophysics, geophysics, chemical engineering and nuclear technology. In particular, attention has been recently focused on this convective process owing to increasing emphasis on the safety of nuclear reactors. The accurate knowledge of thermal convection in a horizontal layer of molten fuel is needed for analyzing the post-accident heat removal problem in a hypothetical core disruptive accident.

Several studies have been done in recent years in the area of thermal convection with volumetric energy sources. For an internally heated fluid layer with an adiabatic lower wall and an isothermal upper wall, works were performed by Tritton and Zarraga [2], Roberts [3], Fiedler and Wille [4], Schwiderski and Schwab [5], and recently by Kulacki and Nagle [6] and Kulacki and Emara [7]. For the case with equal upper and lower surface temperatures, heat transfer studies were conducted by Kulacki and Goldstein [8], Catton and Suo-Anttila [9], and Jahn and Reineke [10]. Recently, some works on a horizontal fluid layer with combined internal and external Rayleigh number effects have been carried out theoretically by Cheung [11] and experimentally by Kikuchi *et al.* [1].

Most of these studies, however, are centered on the macrocharacteristics of mean heat transfer and the overall nature of flow. There are extremely few works on the microcharacteristics of thermal convection, including fluid velocity and temperature fluctuations, which are important for better understanding the mechanism of turbulent heat transport within the fluid layer and are necessary for deriving some heat transfer formulations. To meet this need, the present study has been directed toward the measurement of velocity and temperature fluctuations with turbulent thermal convection in a horizontal layer of water heated internally and from below (combined internal and external heating).

The experimental results will be compared with a simple mixing-length analysis which expresses the turbulent velocity distribution as a function of the relative rates of internal and external heating. In addition, turbulent heat fluxes will be obtained from the measured values of velocity and temperature fluctuations.

EXPERIMENTAL APPARATUS AND PROCEDURE

The apparatus constructed for the present experiments was similar to that of Kikuchi *et al.*[1], with the exception of a laser–Doppler system for velocity measurements (LDV system). The overall dimensions of the fluid layer were 200 × 200 mm, and layer depths were varied from 29 to 96 mm. Four side walls were made of 10-mm-thick acrylic resin plates.

The fluid layer was a dilute aqueous potassium chloride solution. Alternating electric current was passed through the layer vertically from copper plate electrodes, which also served as the upper and lower boundaries of the layer. The layer was also heated from below by a nichrome-resistance bottom heater, which was installed under the lower copper plate. The early bottom heating system was improved to evaluate the surface heat flux more accurately. A compensating heater and a thermal insulator were used to eliminate heat losses from the bottom. The temperature difference between the bottom heater and the compensating heater was measured with thermopiles and maintained near zero with separate power supplies. In this manner the surface heat flux could be calculated, after the steady state had been attained, directly from the electrical power input to the bottom heater.

In order to maintain the upper boundary of the layer at a constant temperature, thermostatically controlled water was circulated into the cooling tank, which was soldered to the back of the upper copper plate.

NOMENCLATURE

a	thermal diffusivity, $\lambda/(\rho c)$
c	specific heat
C_1, C_2	proportionality constants, equations (19) and (25)
f_0, f_1	functions defined in equations (A3) and (A4)
F	flatness factor
g	gravitational acceleration
L	layer depth
m_1, m_2	constant exponents, equations (19) and (25)
$Nu^{\dagger}$	modified Nusselt number, $2q/QL$
Pr	Prandtl number, v/a
q	heat flux
Q	volumetric rate of energy generation
Ra_E	external Rayleigh number, $g\beta\Delta TL^3/av$
Ra_I	internal Rayleigh number, $g\beta QL^5/2\lambda av$
Re	Reynolds number, $w'L/v$
S	skewness factor
T	temperature
ΔT	surface-to-surface temperature difference, $T_0 - T_1$
V	average velocity
w	vertical component of fluid velocity
X	dimensionless distance, z/L
X_c	dimensionless distance defined in equation (11)
z	vertical coordinate, $0 \leqslant z \leqslant L$.

Greek symbols

α_0, α_1	proportionality constants, equations (A1) and (A2)
β	isobaric coefficient of volumetric expansion
θ_b	dimensionless bulk temperature, $(T_b - T_1)/\Delta T$
λ	thermal conductivity
v	kinematic viscosity
ρ	density.

Subscripts

E	external
I	internal
mp	midplane ($X = 0.5$)
0	lower surface
1	upper surface.

Superscripts

$'$	fluctuating component
$\bar{}$	time-averaged
$\tilde{}$	root-mean-square (r.m.s.).

Many chromel–alumel thermocouples were used to monitor the temperatures of copper plates. For measurement of mean and fluctuating temperatures within the layer, a small glass-coated thermocouple (0.3 mm in diameter) was inserted into the fluid layer through the upper boundary.

The fluid velocities were measured using the LDV system, as indicated in Fig. 1. The light beam emitted from a helium–neon laser illuminated a rotating diffraction grating disk, which shifted the beam frequency. Only the first-order diffracted beams, which had a frequency difference of v_s from each other, entered the test fluid and were scattered at the measuring point near the small thermocouple.

In the present apparatus the incident and scattered light beams were symmetric around a vertical axis. The Doppler shift was then a function of the vertical component w' of the fluid velocity. If ψ is the angle of the incoming and the scattered illumination to the horizontal surface, n the index of refraction, and l the vacuum wavelength of the illumination, then the vertical velocity component of the scattering center is given by

$$w' = l(v_D - v_s)/(2n \sin \psi), \tag{1}$$

where v_D is the Doppler shift of the scattered radiation.

To obtain velocity measurements at different positions within the layer, the apparatus containing the fluid layer could be traversed with a three-dimensional movement device. The scattered beam, which passed

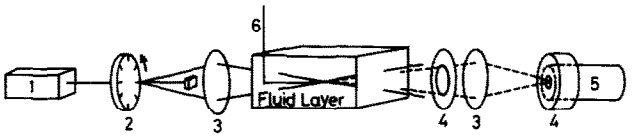

1. He–Ne laser
2. Rotating diffraction grating assembly
3. Lens
4. Aperture
5. Photomultiplier
6. Thermocouple

FIG. 1. Schematic arrangement of laser–Doppler system for velocity measurements.

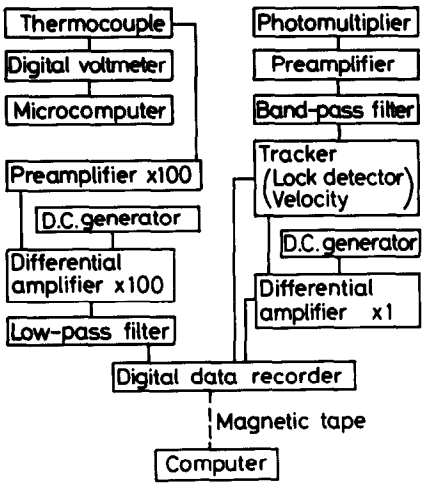

FIG. 2. Block diagram of data processing system.

through the aperture (1 cm in diameter), was focused on the photomultiplier with the receiving lens. The output of the photomultiplier was transmitted to a frequency tracker, which transformed the frequency into the corresponding proportional voltage signal.

A data acquisition and processing system for velocity and temperature signals is shown in Fig. 2. The fluctuation signals were recorded on a digital tape recorder through specially designed measuring circuits. The circuits consisted of a low-noise DC amplifer and a band-pass filter. The recorded signals were played back and then processed with FACOM OS IV/F4 computer system at the Data Processing Center of Kyoto University.

In addition, a visualization technique was used to determine overall flow patterns as well as velocities in the fluid layer. Polystyrene particles were employed as a solid tracer and suspended into the fluid. The illuminations entered the layer through a thin slit, which was attached to the side wall of the convection chamber. Fluid motions in the vertical midplane were recorded on photographs and videotapes.

RESULTS AND DISCUSSIONS

1. *Heat transfer correlation*

In order to establish the basis of the experiments, heat transfer characteristics were first investigated for the combined internal and external heating case. Figure 3 shows the generalized plots of heat transfer data for (a) upper surface and (b) lower surface. The figure also contains the experimental results for other heating cases: external heating and internal heating.

The solid lines drawn in the figure indicate the correlations of Kikuchi *et al.* [1] who compared their experimental results with a boundary-layer analysis and derived the heat transfer correlations

$$Nu_1^{\dagger} Ra_I = 0.201(Ra_E\theta_b)^{1.31}, \tag{2}$$

and

$$Nu_0^{\dagger} Ra_I = 0.257[Ra_E(1-\theta_b)]^{1.31}, \tag{3}$$

where subscripts 1 and 0 denote the upper and the lower surfaces, respectively. $Nu_1^{\dagger}$ and $Nu_0^{\dagger}$ are the modified Nusselt numbers and are defined as

$$Nu_1^{\dagger} = \frac{q_1}{QL/2} \quad \text{and} \quad Nu_0^{\dagger} = \frac{q_0}{QL/2}, \tag{4}$$

where q_1 and q_0 are the heat fluxes at the upper and the lower surfaces, respectively. Q is the internal heat generating rate per unit volume and L the layer depth.

The internal and the external Rayleigh numbers are defined as

$$Ra_I = \frac{g\beta QL^5}{2\lambda a\nu} \quad \text{and} \quad Ra_E = \frac{g\beta\Delta TL^3}{a\nu}, \tag{5}$$

where ΔT is the surface-to-surface temperature difference, $T_0 - T_1$.

The dimensionless bulk core temperature θ_b is defined as $(T_b - T_1)/\Delta T$, where T_b is the bulk core temperature measured at $X(=z/L) = 0.5$.

All the measured values are in good agreement with the correlations of Kikuchi *et al.*, which are expressed by equations (2) and (3). This means that the correlations of Kikuchi *et al.* are applicable not only to

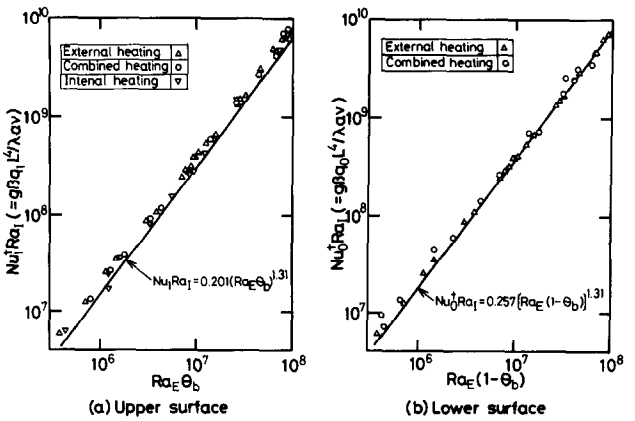

FIG. 3. Comparison of data with generalized heat transfer correlations.

the combined heating case, but to the conventional external and the internal heating cases which are considered as the particular situations in the combined heating case.

2. *Flow visualization*

The photographs in Fig. 4 show flow patterns obtained in the vertical midplane of the convection chamber for different heating cases: (a) external heating, (b) combined heating and (c) internal heating. In each case, the layer depth L was 49 mm and the external Rayleigh number Ra_E about 10^7. Various sizes of vortex are observed in the layer. Some long vertical streaks of particles reveal that the downward-travelling thermals, which are released from the upper boundary, sometimes reach the lower boundary. The same motions do not always persist at certain positions, but the flow pattern is a random process. There are no distinct effects of heating method on the flow pattern.

Visualization gives the overall information of flow motion, but it is difficult to obtain the microcharacteristics of thermal convection. Another technique, i.e. LDV system, was used for direct measurements of local fluid velocity.

3. *Velocity and temperature fluctuations*

Figure 5 shows typical records of vertical velocity (w') and temperature (T') fluctuations, which were measured at several positions for different heating cases: (a) external heating, (b) combined heating and (c) internal heating. In each case, the layer depth was 49 mm, and the heat flux q_1 at the upper surface was

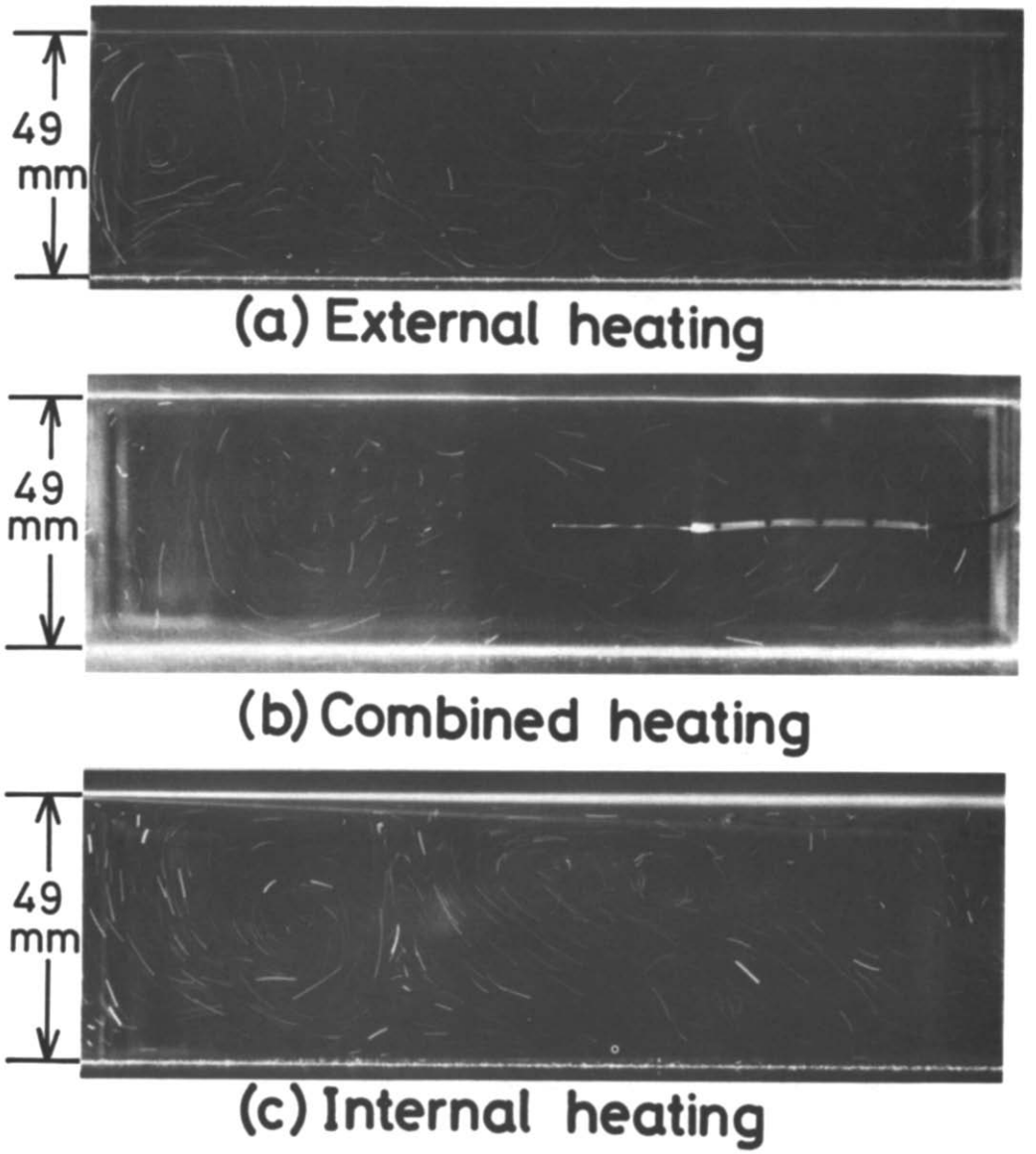

FIG. 4. Photographs of streaklines of flow in convection chamber: (a) external heating, $Ra_E = 9.45 \times 10^6$; (b) combined heating, $Ra_E = 1.45 \times 10^7$, $Ra_I = 5.11 \times 10^7$; (c) internal heating, $Ra_E = 3.81 \times 10^6$, $Ra_I = 5.15 \times 10^7$.

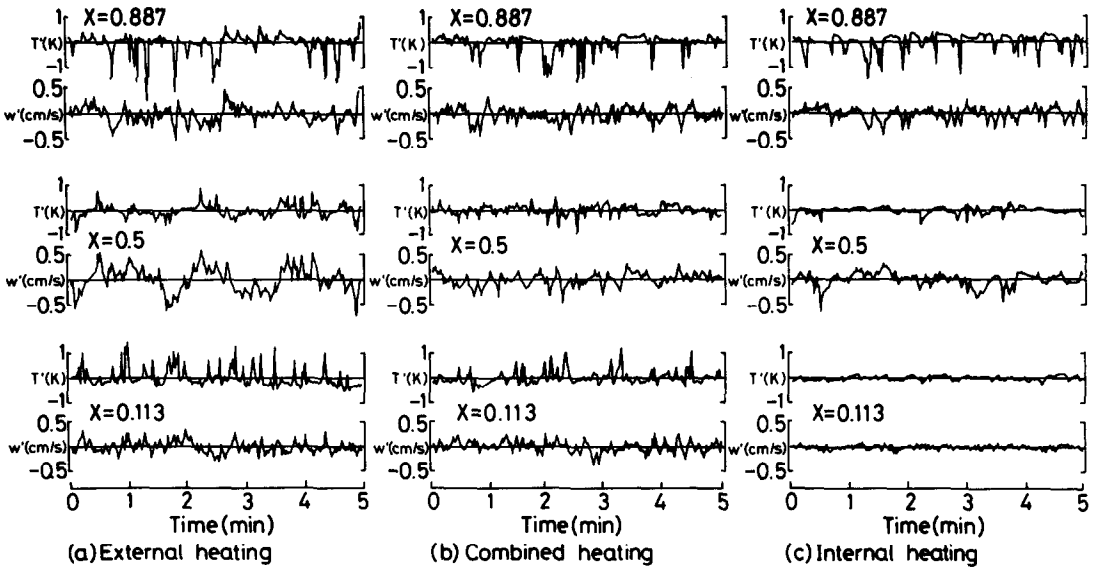

FIG. 5. Typical records of velocity and temperature fluctuations: (a) external heating, $Ra_E = 1.94 \times 10^7$; (b) combined heating, $Ra_E = 1.66 \times 10^7$, $Ra_I = 1.10 \times 10^8$; (c) internal heating, $Ra_E = 1.02 \times 10^7$, $Ra_I = 2.02 \times 10^8$.

about 2×10^3 W m^{-2}. In the central core region ($X = 0.5$) the velocity signals indicate a long-period swell superposed with many ripples while the temperature fluctuations are fairly calm.

In the region near the upper boundary ($X = 0.887$), however, violent spikes of temperature are dominant, which are the rapid drops of temperature accompanied with the intermittent release of cold thermals* from the thermal boundary layer on the upper surface. The release of cold thermals can not be easily determined from the velocity signals since the thermals start to travel at a relatively low velocity.

In the region near the lower boundary ($X = 0.113$), all velocity signals have small fluctuations, but the pattern of temperature fluctuation depends on the heating condition. In the external heating case, violent oscillations are observed which indicate the rapid temperature rises due to the release of hot thermals from the lower thermal boundary layer. In the combined heating case, the oscillations settle down, resulting in a small wavy pattern in the internal heating case.

The above-mentioned fact is indicated more clearly in Fig. 6, which carries plots of the present data in T'–w' space. A symmetrical distribution appears in the central core region, which is nearly isothermal because of strong turbulent mixing. In the regions near the upper and the lower boundaries, however, the distribution is distorted since the cold thermals are intermittently released from the upper thermal boundary layers, while the hot thermals are released from the lower boundary.

In order to compare the probability density function (PDF) of fluctuation signals with a Gaussian distribution, skewness (S) and flatness (F) factors are introduced. S and F of a variable w are defined as

$$S = \overline{w^3}/(\overline{w^2})^{3/2} \quad \text{and} \quad F = \overline{w^4}/(\overline{w^2})^2,$$

where $\overline{\ }$ denotes the average value.† If the PDF has a Gaussian distribution, the values of S and F are 0 and 3, respectively.

Figure 7 shows the skewness and flatness factor distributions of velocity and temperature fluctuations for three different heating cases. In the velocity fluctuation w', S and F have almost constant values of 0 and 3, respectively, at all measuring positions in the layer. There are no distinct effects of heating method on S and F distributions. This means that the PDF of w' is very similar to a Gaussian distribution for each heating case.

In the temperature fluctuations T', however, different distributions of S and F are observed. For the external heating case in which there are no volumetric energy sources, i.e. $Ra_I = 0$, S decreases as the dimensionless distance X increases and has a value of 0 at the midplane ($X = 0.5$) of the layer. When internal heating is added to the layer, i.e. $Ra_I \neq 0$, the situation is quite different. For the combined heating case, the region of negative S value expands and the point where S is zero moves downward from the midplane. For internal heating case, S has a negative value all over the fluid layer.

* A thermal is a mass of fluid, driven by buoyancy, that moves away from a boundary surface into the bulk of the fluid layer.

† A set of data were recorded on a magnetic tape at the speed of 100 samples s^{-1} for approx. 30 min and then, after playback, processed for time-averaging by means of a digital computer. The length of total recording time was sufficiently large for time-averaging since the time records were divided into several shorter sample time records and a reasonably good agreement was confirmed between the average value of the longer sample records and that of the shorter sample records.

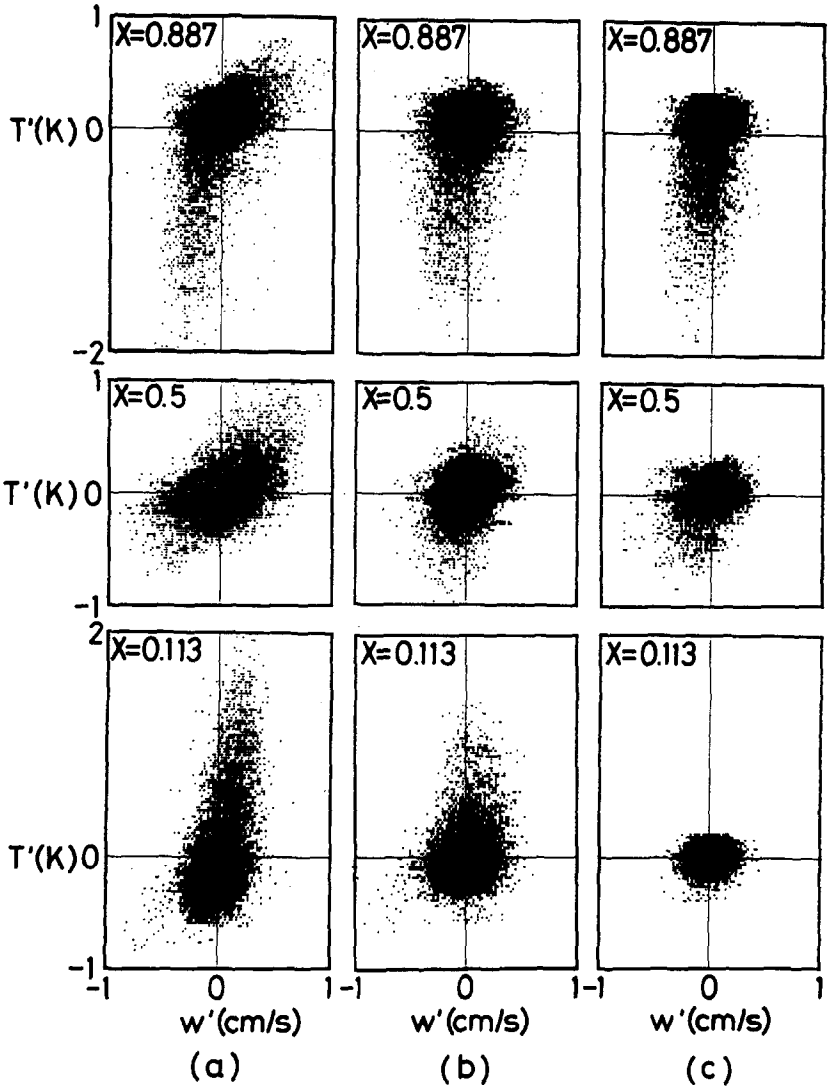

FIG. 6. Correlation between velocity and temperature fluctuations: (a) external heating, $Ra_E = 1.94 \times 10^7$; (b) combined heating, $Ra_E = 1.66 \times 10^7$, $Ra_I = 1.10 \times 10^8$; (c) internal heating, $Ra_E = 1.02 \times 10^7$, $Ra_I = 2.02 \times 10^8$.

The flatness factor of temperature fluctuations is much larger than 3 and the data are scattered.

The above-mentioned fact means that the PDF of T' is different from a Gaussian distribution. This is attributed to the spikes of temperature signals as shown earlier in Fig. 5.

4. *Turbulent velocity and heat flux*

Turbulent convection is characterized by a well-mixed isothermal core region and the intermittent release of thermals from the upper and the lower boundaries. The measurements of vertical velocity w' are, therefore, important for evaluating the energy transport process in thermal convection.

Kraichnan [12] studied analytically the external heating case by a mixing-length approach and indicated that for fluids with high Prandtl numbers such as water the r.m.s. vertical velcoity $\tilde{w}'$ should be proportional to the one-third power of the distance from the wall in the turbulent core region.

Applying Kraichnan's concept to the lower region of the combined heating layer, we first take

$$\tfrac{1}{2}\tilde{w}'^2 \sim \tfrac{1}{2}g\beta z\tilde{T}', \tag{6}$$

where z is the distance from the lower boundary and $\tilde{}$ denotes the r.m.s. value. Equation (6) implies that a typical fluid element which reaches the height z attains a vertical kinetic energy equal to one-half the mean potential energy that would be available from buoyancy if the element had started at $z = 0$ with a temperature excess T' over its surroundings.

Secondly, the mean heat flux is assumed as

$$\tfrac{1}{2}\tilde{w}'\tilde{T}' \sim \frac{q_0}{\rho c} + \frac{Qz}{\rho c}. \tag{7}$$

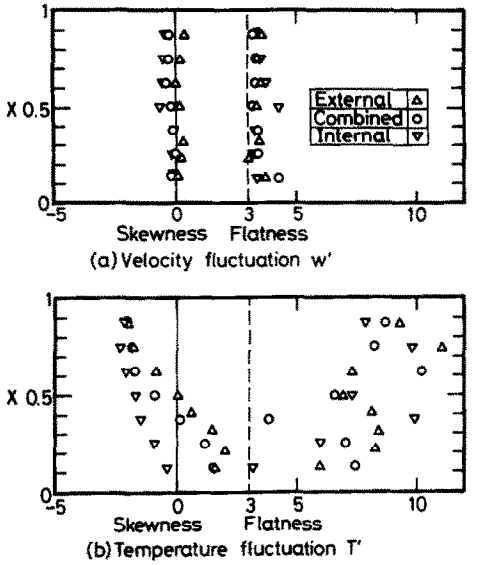

FIG. 7. Skewness and flatness factors of velocity and temperature fluctuations.

The factor $\frac{1}{2}$ expresses an assumption that w' and T' have only a 50% phase correlation.

From equations (6) and (7), the r.m.s. vertical (turbulent) velocity distribution in the lower core region ($0 < X \leqslant X_c$) can be expressed by

$$\tilde{w}' \sim [2g\beta z(q_0+Qz)/(\rho c)]^{1/3} = \left[2\left(\frac{\nu}{L}\right)^3\left(\frac{a}{\nu}\right)^2\left(\frac{g\beta q_0 L^4}{\lambda a \nu}\right)\left(\frac{z}{L}\right)\left(1+\frac{QL}{q_0}\frac{z}{L}\right)\right]^{1/3}.$$

Introducing the dimensionless quantities, we have

$$Re\,Pr^{2/3} \sim [2Nu_0^{\uparrow}Ra_1X(1+2X/Nu_0^{\uparrow})]^{1/3}, \quad (8)$$

where Re and Pr are Reynolds and Prandtl numbers, respectively, and are defined as

$$Re = \frac{\tilde{w}'L}{\nu} \quad \text{and} \quad Pr = \frac{\nu}{a}. \quad (9)$$

Similarly for the upper part of the core region ($X_c < X < 1$), we obtain the kinetic energy and the heat flux by

$$\tfrac{1}{2}\tilde{w}'^2 \sim \tfrac{1}{2}g\beta(L-z)\tilde{T}', \quad \tfrac{1}{2}\tilde{w}'\tilde{T}' \sim \frac{q_1}{\rho c} - \frac{Q(L-z)}{\rho c}.$$

Combination of these equations gives

$$\tilde{w}' \sim \{2g\beta(L-z)[q_1-Q(L-z)]/(\rho c)\}^{1/3} = \left\{2\left(\frac{\nu}{L}\right)^3\left(\frac{a}{\nu}\right)^2\left(\frac{g\beta q_1 L^4}{\lambda a \nu}\right)\left(1-\frac{z}{L}\right)\times\left[1-\frac{QL}{q_1}\left(1-\frac{z}{L}\right)\right]\right\}^{1/3}.$$

Introducing the dimensionless quantities, we have

$$RePr^{2/3} \sim \{2Nu_1^{\uparrow}Ra_1(1-X)[1-2(1-X)/Nu_1^{\uparrow}]\}^{1/3}. \quad (10)$$

If both cold and hot thermals travel vertically through the central core region and lose their identity at $X = X_c (< 0.5)$, X_c may be reasonably determined by

$$X_c \equiv \frac{q_0}{q_0+q_1} = \frac{Nu_0^{\uparrow}}{Nu_0^{\uparrow}+Nu_1^{\uparrow}}. \quad (11)$$

Combination of equations (8) and (10) at $X = X_c$ yields, after rearrangement as shown in the Appendix, the normalized velocity distributions as

$$\frac{\tilde{w}'}{\tilde{w}'_{mp}} = \left[\frac{2X(1+2X/Nu_0^{\uparrow})}{1-1/Nu_1^{\uparrow}}\right]^{1/3} \quad (0 < X \leqslant X_c), \quad (12)$$

and

$$\frac{\tilde{w}'}{\tilde{w}'_{mp}} = \left\{\frac{2(1-X)[1-2(1-X)/Nu_1^{\uparrow}]}{1-1/Nu_1^{\uparrow}}\right\}^{1/3} \quad (X_c < X < 1), \quad (13)$$

where $\tilde{w}'_{mp}$ is the r.m.s. vertical velocity at the midplane ($X = 0.5$) of the fluid layer.

As pointed out earlier, the external and the internal heating cases can be considered as the particular situations in the combined heating case. Equations (12) and (13) will be applied to those particular cases to verify a consistency of turbulent velocity distribution obtained in the combined heating case. In the external heating case q_0 is equal to q_1, i.e. $Nu_0^{\uparrow} = Nu_1^{\uparrow}$. From equation (11) X_c is 0.5. Application of these relations to equation (12) approaches a limit for the velocity distribution in the lower core region:

$$\frac{\tilde{w}'}{\tilde{w}'_{mp}} = \left[\frac{2X(1+2X/Nu_1^{\uparrow})}{1-1/Nu_1^{\uparrow}}\right]^{1/3} \quad (0 < X \leqslant 0.5).$$

By considering that $Q = 0$, i.e. $1/Nu_1^{\uparrow} \to 0$, we finally have

$$\frac{\tilde{w}'}{\tilde{w}'_{mp}} = (2X)^{1/3} \quad (0 < X \leqslant 0.5). \quad (14)$$

Similarly for the upper core region, equation (13) is transformed into a simple form as

$$\frac{\tilde{w}'}{\tilde{w}'_{mp}} = [2(1-X)]^{1/3} \quad (0.5 < X < 1). \quad (15)$$

These correlations of equations (14) and (15) are in good agreement with Kraichnan's prediction [12] for the external heating case.

In the internal heating case, on the other hand, q_0 is zero and q_1 is equal to QL, i.e. $Nu_0^{\uparrow} = 0$ and $Nu_1^{\uparrow} = 2$. From equation (11) we obtain $X_c = 0$. Then the velocity distribution of equation (13) is represented by a simple form all over the core region by

$$\frac{\tilde{w}'}{\tilde{w}'_{mp}} = [4X(1-X)]^{1/3} \quad (0 < X < 1). \quad (16)$$

Figure 8 shows a comparison of these correlations with the present experimental results of velocity distribution, which were obtained in two kinds of fluid layer (49 and 96 mm in depth) for different heating cases: (a) external heating, (b) combined heating and (c)

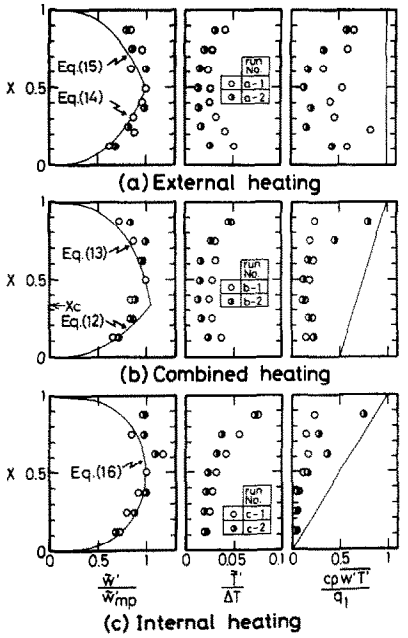

FIG. 8. Distributions of dimensionless velocity, temperature fluctuation and turbulent heat flux.

internal heating. The details of experimental conditions are listed in Table 1. In the external heating case, the velocity has a flat maximum in the central core region and decreases toward zero near the lower and the upper surfaces. Measured values agree fairly well with the theoretical calculations.

In the internal heating case, however, the maximum point moves upward from the midplane and the velocity distribution is then deformed. The experimental results are a little different from the present calculations. This discrepancy is more pronounced in the thinner layer ($L = 49$ mm). A new theory is needed for analyzing the fine structure of flow in the internally heated layer.

In this figure are also indicated the r.m.s. temperature fluctuation $\tilde{T}'$ and the turbulent heat flux $c\rho\overline{\tilde{w}'\tilde{T}'}$, which are normalized by the surface-to-surface temperature difference ΔT $(= T_0 - T_1)$ and the heat flux q_1 at the upper surface, respectively. For the external heating case in which there are no volumetric energy sources, a symmetric distribution of temperature fluctuation with its minimum at the midplane ($X = 0.5$) is dominant. When internal heating is added to the layer, the situation is quite different. In this combined heating case, the minimum point moves downward from the midplane and an asymmetry in the temperature field is occurred. For the internal heating case in which an adiabatic condition is established at the lower surface, there is virtually no minimum point in the core region and the magnitude of temperature fluctuation increases monotonously with increasing X.

The turbulent heat flux, on the other hand, tends to increase with increasing X in the combined heating case as well as in the internal heating case. In the external heating case, however, the experimental data are scattered and no distinct tendency appears in the heat flux distribution. The solid lines drawn in the figure indicate the total heat flux distribution predicted from both external and internal heating rates, which can be related by

$$q = q_0 + QXL. \tag{17}$$

In each case the measured values are lower than the calculations by equation (17). This discrepancy is more pronounced in the central core region since small high-frequency fluctuations of temperature, which are dominant in this region, could not be measured by the thermocouple (0.3 mm in diameter) used in the present experiments. A new instrument such as a finer thermocouple is then required for accurately measuring the high-frequency fluctuations encountered in the core region of the fluid layer. The measured values of turbulent heat flux are also underestimated since there is a little difference between the measuring points of velocity and temperature though the measuring points were brought as close to each other as possible. The systematic underestimation of turbulent heat flux was also reported by Deardorff and Willis [13], who measured the velocity and temperature fluctuations along a horizontal path in air between horizontal plates maintained at constant temperatures.

Although the measured velocity distribution in an internally heated layer is a little different from the theoretical calculation, the mixing-length analysis is possibly applicable to predict, with some degree of accuracy, the r.m.s. vertical velocity $\tilde{w}'_{mp}$ at the midplane of the core region. In order to get the more quantitative validity, the $\tilde{w}'_{mp}$ should be determined. At the midplane X is equal to 0.5 and then equation (10) reduces to

$$Re_{mp}Pr^{2/3} \sim [Nu_1^{\dagger}Ra_1(1 - 1/Nu_1^{\dagger})]^{1/3}, \tag{18}$$

where $Re_{mp} = \tilde{w}'_{mp}L/\nu$.

Table 1. Experimental conditions

Run No.	L (mm)	Ra_E	Ra_I	θ_b	$\tilde{w}'_{mp}$ (cm s^{-1})	ΔT (K)	q_1 (W m^{-2})
a-1	49	1.94×10^7	—	0.5	0.24	7.6	2.0×10^3
a-2	96	1.88×10^8	—	0.5	0.34	8.1	2.1×10^3
b-1	49	1.66×10^7	1.10×10^8	0.66	0.23	6.3	2.1×10^3
b-2	96	1.30×10^8	1.73×10^9	0.68	0.31	6.1	2.0×10^3
c-1	49	1.02×10^7	2.02×10^8	1.0	0.14	3.8	1.9×10^3
c-2	96	8.38×10^7	3.45×10^9	1.0	0.27	3.6	1.9×10^3

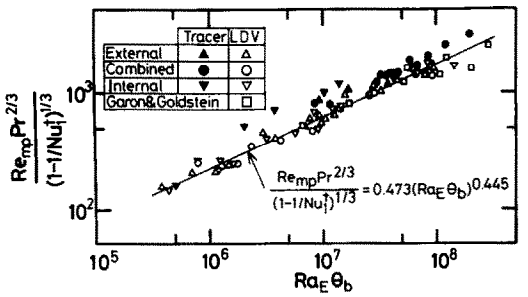

FIG. 9. Generalized turbulent velocity correlation.

Substituting equation (2) into equation (18), we obtain

$$\frac{Re_{mp}Pr^{2/3}}{(1-1/Nu_1^{\uparrow})^{1/3}} \sim 0.738(Ra_E\theta_b)^{0.437}.$$

The proportionality constant and the constant exponent on the RHS of the equation are uncertain and will be directly determined with the use of experimental data in Re_{mp}–Ra_E space by assuming a correlation of the form

$$\frac{Re_{mp}Pr^{2/3}}{(1-1/Nu_1^{\uparrow})^{1/3}} \sim C_1(Ra_E\theta_b)^{m_1}. \tag{19}$$

Figure 9 shows the relationship between $Re_{mp}Pr^{2/3}/(1-1/Nu_1^{\uparrow})^{1/3}$ and $Ra_E\theta_b$ in the present measurements. The experimental data were obtained with two methods: (a) LDV system and (b) tracer method. In the tracer method the r.m.s. vertical velocity was calculated from the following correlation with the assumption of isotropy

$$\tilde{w}'^2 = V^2/3. \tag{20}$$

V was the average velocity which was obtained from several long streaks of moving particles shown in the photographs of Fig. 4.

In Fig. 9 is also indicated the data of Garon and Goldstein [14] for the external heating case. The data of Garon and Goldstein are in good agreement with the present LDV data. The tracer data are a little higher than the LDV data because the average velocity V was obtained from several long streaks of moving particles, as described earlier, and the tracer data were possibly overestimated.

A linear regression of $\ln[Re_{mp}Pr^{2/3}/(1-1/Nu_1^{\uparrow})^{1/3}]$ vs $\ln(Ra_E\theta_b)$ through the present LDV data is

$$\frac{Re_{mp}Pr^{2/3}}{(1-1/Nu_1^{\uparrow})^{1/3}} = 0.473(Ra_E\theta_b)^{0.445}. \tag{21}$$

Consequently, C_1 and m_1 have been well determined as constants. This suggests that the assumption given by equations (6) and (7) is valid for the combined heating case as well as for the external and the internal heating cases.

The generalized correlation of equation (21) has several independent variables and is inconvenient for practical applications. From equations (2)–(4) the parameter $(1-1/Nu_1^{\uparrow})^{1/3}$ on the LHS of equation (21) can be related to the dimensionless bulk core temperature θ_b by

$$\left(1-\frac{1}{Nu_1^{\uparrow}}\right)^{1/3} = \left[\frac{1}{2}\left(1+\frac{q_0}{q_1}\right)\right]^{1/3} = \left\{\frac{1}{2}\left[1+\frac{0.257}{0.201}\left(\frac{1-\theta_b}{\theta_b}\right)^{1.31}\right]\right\}^{1/3}. \tag{22}$$

Substituting equation (22) into (21), we obtain

$$Re_{mp}Pr^{2/3} = 0.473Ra_E^{0.441}f(\theta_b), \tag{23}$$

where

$$f(\theta_b) = \theta_b^{0.445}\left\{\frac{1}{2}\left[1+\frac{0.257}{0.201}\left(\frac{1-\theta_b}{\theta_b}\right)^{1.31}\right]\right\}^{1/3}. \tag{24}$$

$f(\theta_b)$ is varied from 0.767 (at $\theta_b = 0.5$) to 0.794 (at $\theta_b = 1.0$) and maintains almost constant. If $f(\theta_b)$ is assumed to be a constant value, equation (23) can be approximated as

$$Re_{mp}Pr^{2/3} = C_2Ra_E^{m_2}. \tag{25}$$

The constants C_2 and m_2 will be directly determined with the use of experimental data in the Re_{mp}–Ra_E space. Figure 10 shows the relationship between $Re_{mp}Pr^{2/3}$ and Ra_E in the present measurements. A linear regression of $\ln(Re_{mp}Pr^{2/3})$ vs $\ln(Ra_E)$ through the present LDV data is

$$Re_{mp}Pr^{2/3} = 0.305Ra_E^{0.441}. \tag{26}$$

This correlation is very useful for many practical applications since the turbulent velocity can be easily obtained with some degree of accuracy from equation (26) which has only the variables Pr and Ra_E.

CONCLUSIONS

An experimental study has been conducted to investigate the mechanism of turbulent heat transport in a horizontal layer of water heated simultaneously from within and from below. Measurements were taken of the fluid velocity and temperature fluctuations. A visualization technique was also used to determine the overall flow patterns. Comparison of the experimental

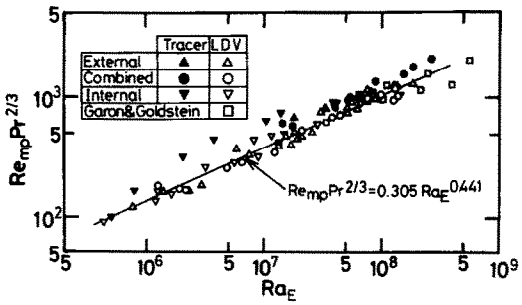

FIG. 10. Simplified turbulent velocity correlation.

results with the mixing-length analysis yielded the following conclusions:

(1) At the edge of the thermal boundary layer the intermittent release of cold and hot thermals plays a major role in the heat transport mechanism. In the central core region, however, strong turbulent mixing is dominant.
(2) Turbulent velocity at the midplane can be easily predicted from equation (26) which has only the variables Pr and Ra_E. But the experimental results of velocity distribution are a little different from the prediction of the mixing-length analysis. A new theory is needed for analyzing the fine structure of turbulent flow, especially in the internally heated layer.
(3) The measured turbulent heat flux is lower than the total heat flux calculated from both internal and external heating rates. This discrepancy is more pronounced in the central core region since small high-frequency fluctuations of temperature cannot be measured by the present thermocouple. A new instrument is required for the more accurate measurement of temperature fluctuations.

Acknowledgements—The authors with to express their thanks to Professor I. Michiyoshi, Kyoto University, for his support and encouragement throughout the study. Thanks are also due to Assistant Professor T. Nakajima, Kobe University, for his valuable suggestions of the laser–Doppler system. The authors were favored with the assistance of Mr T. Hori who helped perform the experiments.

REFERENCES

1. Y. Kikuchi, T. Kawasaki and T. Shioyama, Thermal convection in a horizontal fluid layer heated internally and from below, *Int. J. Heat Mass Transfer* **25,** 363–370 (1982).
2. D. J. Tritton and M. N. Zarraga, Convection in horizontal fluid layers with heat generation experiments, *J. Fluid Mech.* **30,** 21–32 (1967).
3. P. L. Roberts, Convection in horizontal fluid layers with heat generation theory, *J. Fluid Mech.* **30,** 33–41 (1967).
4. H. E. Fiedler and R. Wille, Turbulente Freie Konvektion in Einer Horizontalen Flüssigkeitsschicht mit Volumen-Wärmequelle, Paper NC4.5, *Proc. 4th Int. Heat Transfer Conference*, Paris (1970).
5. E. W. Schwiderski and H. J. A. Schwab, Convection experiments with electrolytically heated fluid layers, *J. Fluid Mech.* **48,** 703–719 (1971).
6. F. A. Kulacki and M. Z. Nagle, Natural convection in a horizontal fluid layer with volumetric energy sources, *J. Heat Transfer* **97,** 204–211 (1975).
7. F. A. Kulacki and A. A. Emara, Heat transfer correlations for use in PAHR analysis and design, *Trans. Am. nucl. Soc.* **22,** 447–448 (1975).
8. F. A. Kulacki and R. J. Goldstein, Thermal convection in a horizontal fluid layer with uniform volumetric energy sources, *J. Fluid Mech.* **55,** 271–287 (1972).
9. I. Catton and A. J. Suo-Anttila, Heat transfer from a volumetrically heated horizontal fluid layer, Paper NC2.7, *Proc. 5th Int. Heat Transfer Conference*, Tokyo (1974).
10. M. Jahn and H. H. Reineke, Free convection heat transfer with internal heat sources, calculations and measurements, Paper NC2.8, *Proc. 5th Int. Heat Transfer Conference*, Tokyo (1974).
11. F. B. Cheung, Correlation equations for turbulent thermal convection in a horizontal fluid layer heated internally and from below, *J. Heat Transfer* **100,** 416–422 (1978).
12. R. H. Kraichnan, Turbulent thermal convection at arbitrary Prandtl number, *Phys. Fluids* **5,** 1374–1389 (1962).
13. J. W. Deardorff and G. E. Willis, Investigation of turbulent thermal convection between horizontal plates, *J. Fluid Mech.* **28,** 675–704 (1967).
14. A. M. Garon and R. J. Goldstein, Velocity and heat transfer measurements in thermal convection, *Phys. Fluids* **16,** 1818–1825 (1973).

APPENDIX

Equations (8) and (10) can be transformed into the following forms by

$$RePr^{2/3} = \alpha_0 f_0(X) \quad (0 < X \leqslant X_c), \tag{A1}$$

$$RePr^{2/3} = \alpha_1 f_1(X) \quad (X_c < X < 1). \tag{A2}$$

where α_0 and α_1 are the proportionality constants. $f_0(X)$ and $f_1(X)$ are defined as

$$f_0(X) \equiv [2Nu_0^{\dagger} Ra_I X(1+2X/Nu_0^{\dagger}]^{1/3}, \tag{A3}$$

$$f_1(X) \equiv \{2Nu_1^{\dagger} Ra_I(1-X)[1-2(1-X)/Nu_1^{\dagger}]\}^{1/3}. \tag{A4}$$

Combination of equations (A1) and (A2) at $X = X_c$ yields

$$\frac{\alpha_0}{\alpha_1} = \frac{f_1(X_c)}{f_0(X_c)}.$$

Introducing equations (A3), (A4) and (11), we have

$$\frac{\alpha_0}{\alpha_1} = \left\{\frac{Nu_1^{\dagger 2}[1-2/(Nu_0^{\dagger}+Nu_1^{\dagger})]}{Nu_0^{\dagger 2}[1+2/(Nu_0^{\dagger}+Nu_1^{\dagger})]}\right\}^{1/3} = \left(\frac{Nu_1^{\dagger}}{Nu_0^{\dagger}}\right)^{1/3}, \tag{A5}$$

where the relation that $q_1 - q_0 = QL$, i.e. $Nu_1^{\dagger} - Nu_0^{\dagger} = 2$, has been used.

The midplane is contained within the upper part of the core region ($X_c < X < 1$) since X_c is less than 0.5. By the use of the midplane velocity $\tilde{w}'_{mp}$, equation (A2) can be transformed into a normalized form as

$$\frac{\tilde{w}'}{\tilde{w}'_{mp}} = \frac{RePr^{2/3}}{Re_{mp}Pr^{2/3}} = \frac{f_1(X)}{f_1(0.5)} = \left\{\frac{2(1-X)[1-2(1-X)/Nu_1^{\dagger}]}{1-1/Nu_1^{\dagger}}\right\}^{1/3} \quad (X_c < X < 1). \tag{A6}$$

In the lower part of the core region ($0 < X \leqslant X_c$), however, the normalized velocity distribution is expressed by

$$\frac{\tilde{w}'}{\tilde{w}'_{mp}} = \frac{\alpha_0 f_0(X)}{\alpha_1 f_1(0.5)}. \tag{A7}$$

Substituting equations (A3)–(A5) into (A7), we have, after some manipulations,

$$\frac{\tilde{w}'}{\tilde{w}'_{mp}} = \left[\frac{2X(1+2X/Nu_0^{\dagger})}{1-1/Nu_1^{\dagger}}\right]^{1/3} \quad (0 < X \leqslant X_c). \tag{A8}$$

TRANSFERT THERMIQUE TURBULENT DANS UNE COUCHE FLUIDE HORIZONTALE CHAUFFEE INTERIEUREMENT ET PAR LE BAS

Résumé—Des mesures de fluctuations de vitesse et de température sont faites pour la convection thermique turbulente dans une couche horizontale d'eau avec des sources volumiques d'énergie uniformes et un flux constant de chauffage par le bas. Les données expérimentales sont comparées avec une analyse simple de longueur de mélange et une équation est donnée pour la vitesse turbulente au plan médian de la couche fluide. Le flux thermique turbulent, obtenu à partir des valeurs mesurées de fluctuations de vitesse et de température, est plus faible que le flux thermique total prédit par les flux de chauffage interne et externe.

TURBULENTER WÄRMETRANSPORT IN EINER HORIZONTALEN INTERN UND EXTERN BEHEIZTEN FLUIDSCHICHT

Zusammenfassung—Es wurden Messungen der Schwankungen von Fluidgeschwindigkeit und -temperatur bei turbulenter thermischer Konvektion in einer horizontalen Wasserschicht mit gleichförmigen volumetrischen Wärmequellen und konstanter Beheizung von unten durchgeführt. Die experimentellen Daten wurden mit einer einfachen Analyse der Mischungslänge verglichen. Für die turbulente Geschwindigkeit in der Mittenebene der Fluidschicht wurde eine Korrelationsgleichung formuliert. Die aus den gemessenen Schwankungswerten von Geschwindigkeit und Temperatur ermittelte turbulente Wärmestromdichte ist geringer als die gesamte Wärmestromdichte, die sich aus der Summe der internen und externen Wärmequellen berechnet.

ТУРБУЛЕНТНЫЙ ТЕПЛОПЕРЕНОС В ГОРИЗОНТАЛЬНОМ СЛОЕ ЖИДКОСТИ С ВНУТРЕННИМИ ТЕПЛОВЫМИ ИСТОЧНИКАМИ И ПОДОГРЕВОМ СНИЗУ

Аннотация—Измерены флуктуации скорости и температуры при турбулентной тепловой конвекции в горизонтальном слое воды с однородными объемными источниками энергии и подводимым снизу постоянным тепловым потоком. Экспериментальные данные сравниваются с результатами простого анализа с использованием гипотезы длины пути смешения и корреляционного уравнения, полученного для турбулентной скорости в средней части слоя жидкости. Турбулентный тепловой поток, найденный по измеренным значениям флуктуаций скорости и температуры, был ниже, чем общий тепловой поток, рассчитанный по скорости внутреннего и внешнего нагрева.